Available online at www.sciencedirect.com
SCIENCE DIRECT®
C. R. Chimie 6 (2003) 135–145
COMPTES RENDUS CHIMIE

Account / Revue

Exchange and correlation effects in transition-metal oxides $3d^n$ (n = 4, 5 and 6)

Michel Pouchard, Antoine Villesuzanne, Jean-Pierre Doumerc *

ICMCB–CNRS, 87, avenue du Docteur-Albert-Schweitzer, 33608 Pessac, France

Received 4 November 2002; accepted 26 December 2002

Abstract

In order to clarify the competition of exchange and correlation energies vs crystal-field stabilisation energy, a simple approach is proposed. The exchange and correlation contributions are described on the base of Brandow and Kanamori's U, U' and J_H parameters. The dependence of the crystal field effect on site distortion has simply been modelled using a linear interpolation between undistorted and fully distorted sites. This approach leads to establish phase diagrams for d^4, d^5 and d^6 cations, allowing us to predict the spin-state stability range depending on exchange (J_H), crystal field (Dq) and distortion (k) parameters. It can be used to complement the Extended Hückel Tight Binding calculations of the electronic structure of materials having a noticeable ionic character such as 3d transition-metal oxides, in order to interpret the electronic behaviour, and, particularly, discuss the insulating-vs-metallic character of these oxides. ***To cite this article: M. Pouchard et al., C. R. Chimie 6 (2003) 135–145.***

Résumé

Afin de mieux comprendre la compétition qui oppose les effets d'échange et de corrélation à ceux du champ cristallin, une approche simple est proposée. Les contributions d'échange et de corrélation sont décrites sur la base des paramètres U, U' et J_H de Brandow et Kanamori. L'évolution de la contribution du champ cristallin avec la distorsion du site a été simplement modélisée à l'aide d'une interpolation linéaire entre le site non distordu et complètement distordu. Cette approche conduit à l'établissement de diagrammes de phase pour les cations d^4, d^5 et d^6, permettant de prévoir le domaine de stabilité d'un état de spin en fonction des paramètres d'échange (J_H), de champ cristallin (Dq) et de distorsion (k). Elle peut être utilisée pour compléter les calculs de structure électronique de type liaison forte Hückel étendue dans le cas de matériaux ayant un caractère ionique notable, tels que les oxydes d'éléments de transition, dans le but d'interpréter le comportement électronique et, en particulier, de discuter le caractère isolant ou métallique de ces oxydes. ***Pour citer cet article : M. Pouchard et al., C. R. Chimie 6 (2003) 135–145.***

Keywords: exchange; correlation; crystal field; transition metal oxides; electronic structure; metal–insulator transitions; spin-state phase diagrams

Mots clés : échange ; corrélation ; champ cristallin ; oxydes d'éléments de transition ; structure électronique ; transitions métal–isolant ; diagrammes de phase d'états de spin

* Corresponding author.

E-mail addresses: pouchard@icmcb.u-bordeaux.fr (M. Pouchard), ville@icmcb.u-bordeaux.fr (A. Villesuzanne), doumerc@icmcb.u-bordeaux.fr (J.-P. Doumerc).

DOI: 10.1016/S1631-0748(03)00014-6

1. Introduction

Exchange and correlation phenomena describe the effects of electron–electron interactions beyond the one-electron mean-field approximation; they are necessary to build correct electronic configurations based on an orbital description for $3d^n$ ions. A large part of the correlation energy, in the sense of electron–electron interactions, is included in mean-field approaches: for example, most one-electron schemes account for screening phenomena (i.e. Slater screening constant). In the Hartree–Fock framework, correlation energy is defined restrictively as the difference between the exact and the Hartree–Fock ground-state energy.

Exchange phenomena are more complex, including the symmetry of the wave functions and the Fermi hole, both giving rise to Hund's rules [1]. In the case of partially occupied orbitals, for example 3d orbitals for transition metals, exchange will contribute to differentiate up- and down-spin populations.

In inorganic molecular chemistry, exchange and correlation are discussed on the basis of Racah *A*, *B*, *C*, or Slater parameters, which allow to quantify electron–electron interactions and result in the Tanabe–Sugano diagrams for octahedral complexes. What about solid-state chemistry?

Tight-binding methods as Extended Hückel (EHTB), which emphasise atomic orbital overlaps, do not include exchange and correlation effects. Moreover, in non self-consistent methods as EHTB, crystal or molecular orbital energies do not depend on the electron count.

Methods based on the Density Functional Theory (DFT) use approximate exchange-correlation functionals (so-called LDA, GGA, WDA...), based on the analytical expression for the exchange-correlation energy of an homogenous electron gas. Although closer to the exact energy than single-determinant Hartree–Fock, DFT remains at the mean-field stage. A step beyond correlation effects can be achieved through the LDA+U method, in which on-site electron–electron repulsion terms are added to the exchange-correlation functional [2].

Chemical bonding in transition metal oxides can be described on the basis of two types of atomic orbitals:

- (*i*) s and p orbitals, for which ζ Slater exponents take low values ($\zeta_{4s} \sim$ 1–1.5 [3]), corresponding to diffuse orbitals;
- d orbitals, more localised ($\zeta_{3d} \sim$ 2.5–4.5 [3]), describing strongly interacting electrons, for which exchange and correlation phenomena are often crucial.

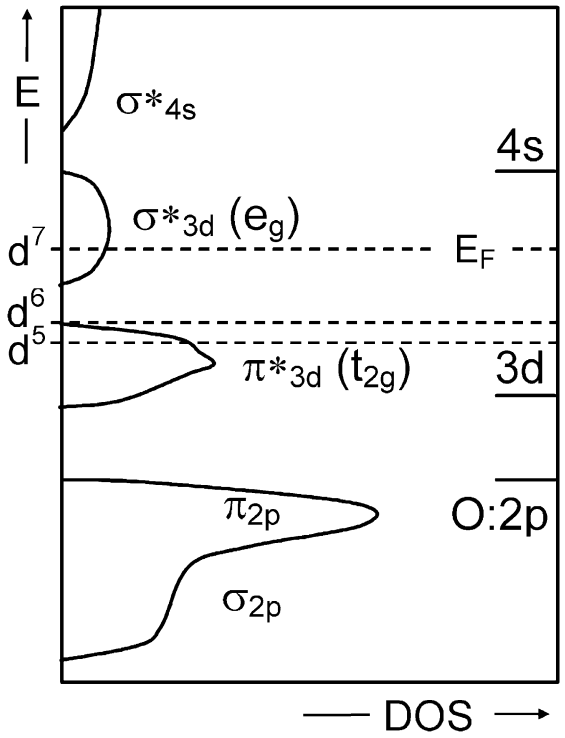

Fig. 1. Schematic monoelectronic band structure for a cubic perovskite $LaMO_3$(M = d^5, d^6, and d^7 cation) on the basis of EHTB method.

As an example, a monoelectronic band description of the three following double oxides with rhombohedral perovskite-related structures would predict a metallic behaviour for $LaFeO_3$ (d^5) and $LaNiO_3$ (d^7), and an insulating one for $LaCoO_3$ (d^6) (Fig. 1). Whereas $LaNiO_3$ indeed is a metal at any temperatures (within its stability range), $LaFeO_3$ actually is always insulating and $LaCoO_3$ undergoes an insulating to metal transition at high temperature. So a simple low-spin band description, neglecting exchange and correlation effects, does not correspond to experimental facts.

In $LaFeO_3$, trivalent iron ($3d^5$) is not in the low-spin $t_{2g}^5e_g^0$ configuration (favoured by the crystal field), but in the high-spin $t_{2g}^3e_g^2$ configuration (favoured by exchange and correlation). The competition between crystal field (which stabilises some energy levels) and exchange and correlation (which tend to keep electrons apart in space) is at the origin of spin equilibria and

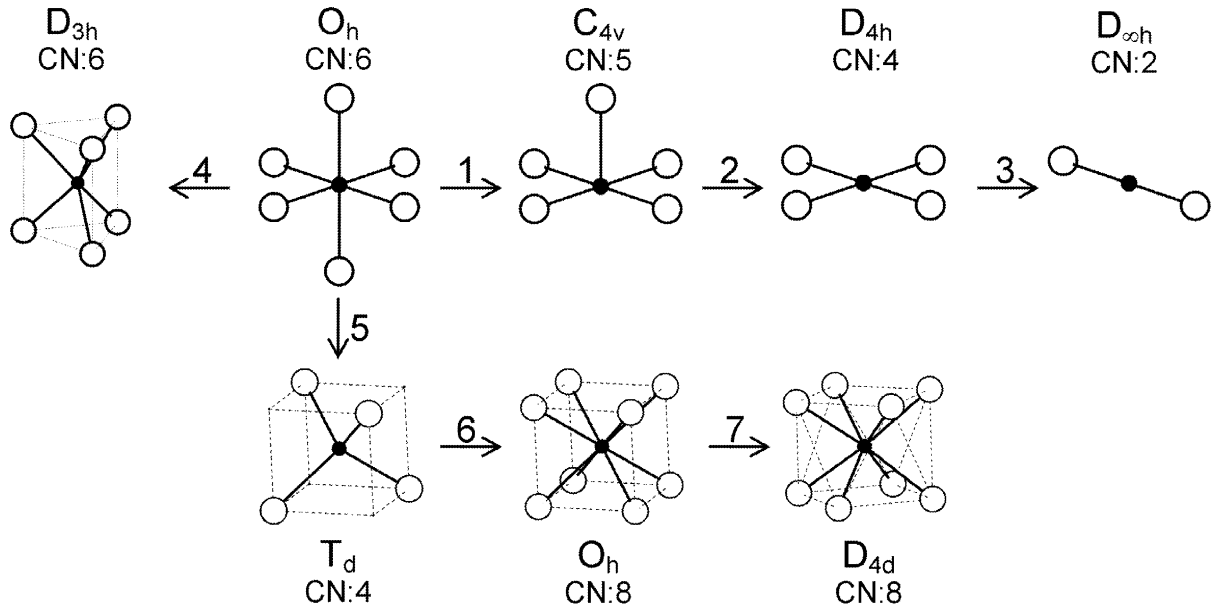

Fig. 2. Various coordinations and symmetries of cationic sites in oxides.

spin transition phenomena. At low temperature, the six 3d electrons of cobalt in $LaCoO_3$ lie in the three low-lying t_{2g} orbitals, giving an insulating state; at high temperature, exchange and correlation prevail and spread the six electrons in the five d orbitals. Then $LaCoO_3$ becomes a metal, with the cobalt ion in an intermediate spin state.

In the following, we will describe exchange and correlation effects for transition metal ions in various coordination polyhedra the symmetry of which strongly influences the energy splitting of the five 3d orbitals. We will extend the treatment of most-common octahedral (O_h) and tetrahedral (T_d) sites to the square-based pyramidal (C_{4v}), square planar (D_{4h}), dumbbell ($D_{\infty h}$), cubic (O_h) and antiprismatic (D_{4d}) environments (Fig. 2).

We will restrict our discussion to d^4, d^5 and d^6 ions, most interesting because they are to be found in three different spin states: $S = 0$, 1 and 2 for d^4 and d^6 ions; $S = 1/2$, 3/2 and 5/2 for the d^5 ion. Our approach can then be applied to metal ions such as, for example, Fe^{4+} and Mn^{3+} ($3d^4$), Fe^{3+} and Co^{4+} ($3d^5$), Co^{3+} ($3d^6$). Its extension to the 4d and 5d series should be handled cautiously because of the spin–orbit coupling.

The aim of this work is to guide inorganic chemists in the choice of appropriate crystal structures for stabilising a chosen electronic configuration for these 3d transition ions, and to help in the interpretation of their remarkable physical properties.

2. Expression of the exchange and correlation using U, U' and J_H parameters of Kanamori and Brandow

According to Kanamori [4] and Brandow [5], Coulomb repulsion energy between two electrons belonging to the same atomic orbital (U) or to two different orbitals (U') is balanced by an exchange energy (J_H) that stabilises parallel vs antiparallel spins. These parameters are expressed by the following integrals:

$$U = <\mu\mu|V|\mu\mu> \,,\; U' = <\mu\mu'|V|\mu\mu'>$$

$$\text{and} \quad J_H = <\mu\mu'|V|\mu'\mu>$$

where μ and μ' are different 3d orbitals from a single site and V is the Coulomb operator.

These energies are linked to Racah parameters through the following relationships [5]:

$$U = A + 4B + 3C,\; U' = A - B + C$$

$$\text{and} \quad J_H = 5/2\, B + C$$

These relationships show that U, U' and J_H are not independent and immediately lead to $U - U' = 2\, J_H$,

which will allow us to compare the energy of the various spin states using a single parameter, the Hund's rule exchange energy, J_H. For a $3d^4$ ion in an octahedral site and a HS configuration ($t_{2g}^3 e_g^1$), the energy of a singly occupied (so) e_g orbital can be written as:

$$E^{so}_{e_g} = E_{core} + 3\,U' - 3\,J_H + 6\,Dq$$

where E_{core} stands for the interaction of the 3d electrons with the nucleus and the [Ar] core electrons, and Dq is the crystal field parameter. The three t_{2g} electrons are lying at the energy:

$$E^{so}_{t_{2g}} = E_{core} + 3\,U' - 3\,J_H - 4\,Dq$$

Summing the crystal field energy over the four electrons and taking half the sum of exchange and correlation energies (as each contribution is shared by two electrons), the ion overall energy (E_T), including nucleus–electron and electron–electron interactions, becomes:

$$E_T = 4\,E_{core} + 3/2\,(3\,U' - 3\,J_H) + 1/2\,(3\,U' - 3\,J_H) - 3 \times 4\,Dq + 6\,Dq = 4\,E_{core} + 6\,U' - 6\,J_H - 6\,Dq$$

The so-called t_{2g}^4($S = 1$) low spin (LS) state actually is an intermediate spin (IS) state, but in no case the $S = 0$ state can be the ground state in an octahedral site of O_h symmetry owing to the Hund's rule. Depending on whether the site is singly (so) or doubly occupied (do) and whether the spin is a majority (denoted α) or minority (denoted β) one, the electron energies respectively are:

$$E^{\alpha so}_{t_{2g}} = E_{core} + 3\,U' - 2\,J_H - 4\,Dq$$

$$E^{\alpha do}_{t_{2g}} = E_{core} + U + 2\,U' - 2\,J_H - 4\,Dq$$

$$E^{\beta do}_{t_{2g}} = E_{core} + U + 2\,U' - 4\,Dq$$

In the same way as above, we obtain for the total energy:

$$E_T = 4\,E_{core} + U + 5\,U' - 3\,J_H - 16\,Dq$$

It should be pointed out that in a T_d tetrahedral site where the e orbitals are stabilised by –2.67 Dq and t_2 orbitals are lifted by 1.78 Dq, the e^4 LS ($S = 0$) configuration reversely becomes stable vs the $S = 1$ state. The energy of an electron belonging to one of the two doubly occupied degenerate e-orbitals (as there is the same number of spin up and spin down electrons) is:

$$E^{\alpha do}_{e} = E^{\beta do}_{e} = E_{core} + U + 2\,U' - J_H - 2.67\,Dq$$

and the total energy is:

$$E_T = 4\,E_{core} + 2\,U + 4\,U' - 2\,J_H - 10.68\,Dq$$

Making equal the E_T energies of the HS ($S = 2$) and IS ($S = 1$) states of a d^4 ion in O_h symmetry leads to $J_H/Dq = 2$. For high values of J_H, the HS state is stable and for high values of Dq the IS state on the contrary becomes the ground state.

In T_d symmetry, the condition for passing from $S = 2$ to $S = 0$ becomes $J_H/Dq = 1.1125$.

For the $d^5$and d^6 cations, the IS state ($S = 3/2$ or $S = 1$, respectively) is unstable in O_h symmetry from the following conditions: in the d^5 case, the LS→IS transition requires $J_H/Dq > 5/2$, but the IS→HS transition requires only $J_H/Dq > 5/3$. Therefore, one predicts a direct LS→HS transition which is actually expected for $J_H/Dq > 2$. In the d^6 case, the LS→IS transition requires $J_H/Dq > 10/3$, the IS→HS transition only $J_H/Dq > 2$. The direct LS→HS transition occurs at $J_H/Dq > 2.5$.

3. Influence of a structural distortion on spin transitions of a d^4 ion

Let us first consider the case in which one of the six oxygen atoms moves away from the central ion, the coordination progressively changing from octahedral of O_h symmetry to a (5 + 1) coordination of C_{4v} symmetry until the limiting case of the square based pyramid is reached. In this type of coordination, a simple crystal field approach gives the following energy values in Dq units for the five d orbitals [6]:

$$E^{C_{4v}}_{z^2} = +0.86,\ E^{C_{4v}}_{x^2-y^2} = +9.14,\ E^{C_{4v}}_{xy} = -0.86,\ E^{C_{4v}}_{xz} = E^{C_{4v}}_{xz} = -4.57$$

In octahedral (O_h) coordination:

$$E^{O_h}_{z^2} = E^{O_h}_{x^2-y^2} = +6,\ E^{O_h}_{xy} = E^{O_h}_{xz} = E^{O_h}_{yz} = -4$$

We assume that the magnitude of the distortion can be measured by a coefficient k ($0 \le k \le 1$) and that the energy of the orbital i is a function of k:

$$E_i(k) = (1 - k)\, E_i(0) + k\, E_i \qquad (1)$$

where $E_i(0)$ is the energy of the orbital i in the undistorted site and $E_i(1)$ the energy in the fully distorted site.

For instance, in the present case, with $E_i(0) = E_i^{O_h}$ and $E_i(1) = E_i^{C_{4v}}$, we obtain:

$$E_{z^2} = (6 - 5.14\,k)\,Dq,\ E_{x^2-y^2} = (6 + 3.14\,k)\,Dq$$

$$E_{xy} = (-4 + 3.14\,k)\,Dq,\ E_{xz} = E_{yz} = (-4 - 0.57\,k)\,Dq$$

Using these energy values $E_i(k,Dq)$ to take into account the crystal field effect in the computation of the atomic orbital energies including the exchange correlation effects and then in the computation of the overall energy of the ion for each configuration, the following relations are obtained for the three possible spin equilibria:

$$S = 2 \leftrightarrow S = 1 \quad J_H/Dq = 2 - 0.914\,k$$

$$S = 1 \leftrightarrow S = 0 \quad J_H/Dq = 1.237\,k$$

$$S = 2 \leftrightarrow S = 0 \quad J_H/Dq = 1.25 - 0.1075\,k$$

It is now possible to delimit in a J_H/Dq-vs-k diagram the existence domains of each electronic configuration, $S = 2$, $S = 1$ and $S = 0$ (Fig. 3).

The three straight lines intercept at a triple point t of abscissa k_t where the three spin states are simultaneously stable ($k_t = 0.923$ and $J_H/Dq = 1.142$). As usual, if we look for the more stable state, only three half-line starting from t correspond to an actual equilibrium. As already pointed out, $S = 0$ cannot be stable in O_h symmetry. On the other hand, $S = 1$ cannot exist beyond the k value of 0.923. We can extend the calculations of the crystal field contribution to the five 3d atomic orbitals to the seven types of distortions illustrated in Fig. 2, which encompasses most of the crystal

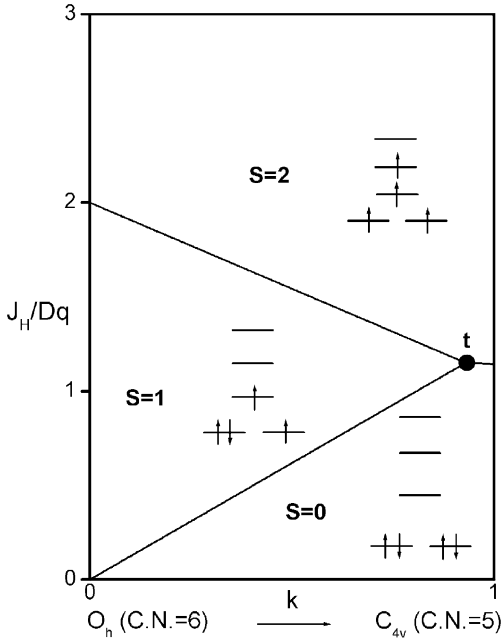

Fig. 3. Spin-state phase diagram for a d^4 ion in C_{4v} symmetry depending on exchange (J_H), crystal field (Dq) and distortion (k) parameters.

sites usually observed in transition metal oxides. In cases (4) and (7), k represents a rotation from 0 to 60° and from 0 to 45°, respectively. Case (5) corresponds to a hypothetic case progressively passing from an octahedron (CN = 6) to a tetrahedron (CN = 4). The orbital energies are given in Table 1. The J_H/Dq-vs-k diagrams are given for each spin state in Figs. 4–6, for $3d^4$, $3d^5$, and $3d^6$ ions, respectively. These diagrams show that, whereas in O_h symmetry no value of J_H/Dq allows to stabilise the three possible spin states of the d^4, d^5 and d^6 ions – at least for narrow d levels –, most of the distortions (C_{4v}, D_{4h}, $D_{\infty h}$, D_{3h}, D_{4d}) allow it, with one triple point t or even two triple points t_1 and t_2. For a d^4 ion in D_{4h} symmetry (i.e. an octahedron distorting into

Table 1
Energies (in Dq units) of the five d orbitals for the site distortions illustrated in Fig. 2.

	d_{z^2}	$d_{x^2-y^2}$	d_{xy}	$d_{xz,yz}$
C_{4v}	6 – 5.14 k	6 + 3.14 k	–4 + 3.14 k	–4 – 0.57 k
D_{4h}	6 – 10.28 k	6 + 6.28 k	–4 + 6.28 k	–4 – 1.14 k
$D_{\infty h}$	6 + 4.28 k	6 – 12.28 k	–4 – 2.28 k	–4 + 5.14 k
D_{3h}	6 – 5.04 k	6 – 11.84 k	–4 – 1.84 k	–4 + 9.36 k
T_d (hyp.)	6 – 8.67 k	6 – 8.67 k	–4 + 5.78 k	–4 + 5.78 k
O_h (CN8)	–2.67 – 2.67 k	–2.67 – 2.67 k	1.78 + 1.78 k	1.78 + 1.78 k
D_{4d}	–5.34	–5.34 + 4.45 k	3.56 – 4.45 k	3.56

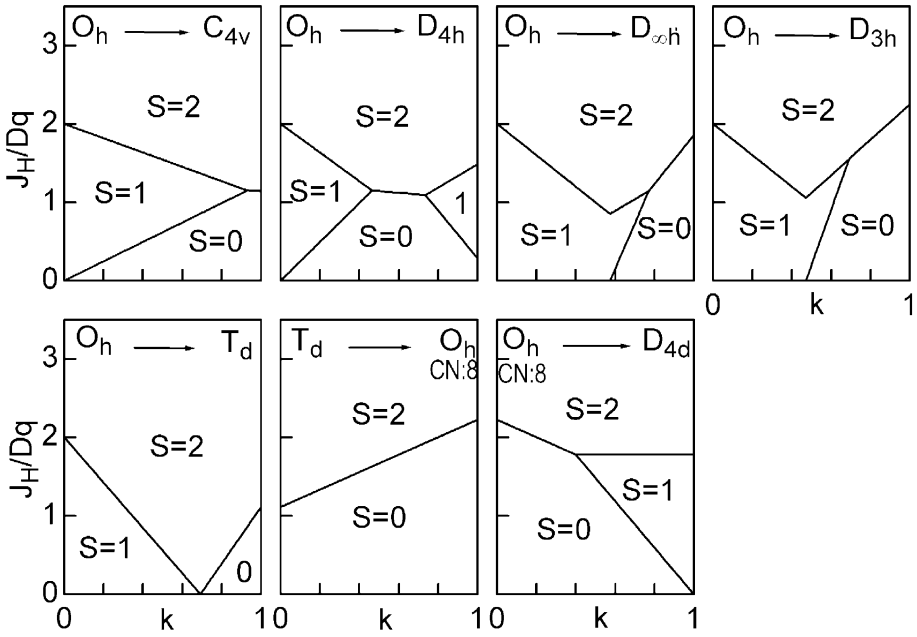

Fig. 4. Spin-state phase diagram for a d^4 ion in the various symmetry sites shown in Fig. 2.

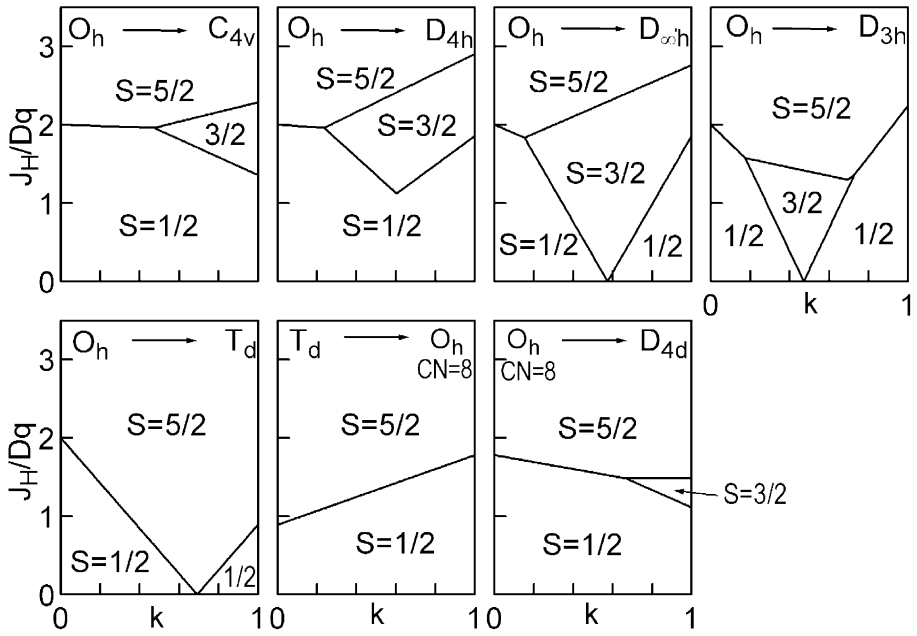

Fig. 5. Spin-state phase diagram for a d^5 ion in the various symmetry sites shown in Fig. 2.

a square) $k_{t1} = 0.465$ and $k_{t2} = 0.735$, and for a d^5 ion in D_{3h} symmetry (i.e. an octahedron distorting into a triangle based prism), $k_{t1} = 0.175$ and $k_{t2} = 0.728$. Some diagrams exhibit particular points of abscissa k_c generally corresponding to the energy crossover of some atomic orbitals as k varies. Let us finally notice that predicted spin transitions are occurring for J_H/Dq values close to 2 (±0.5). As according to literature,

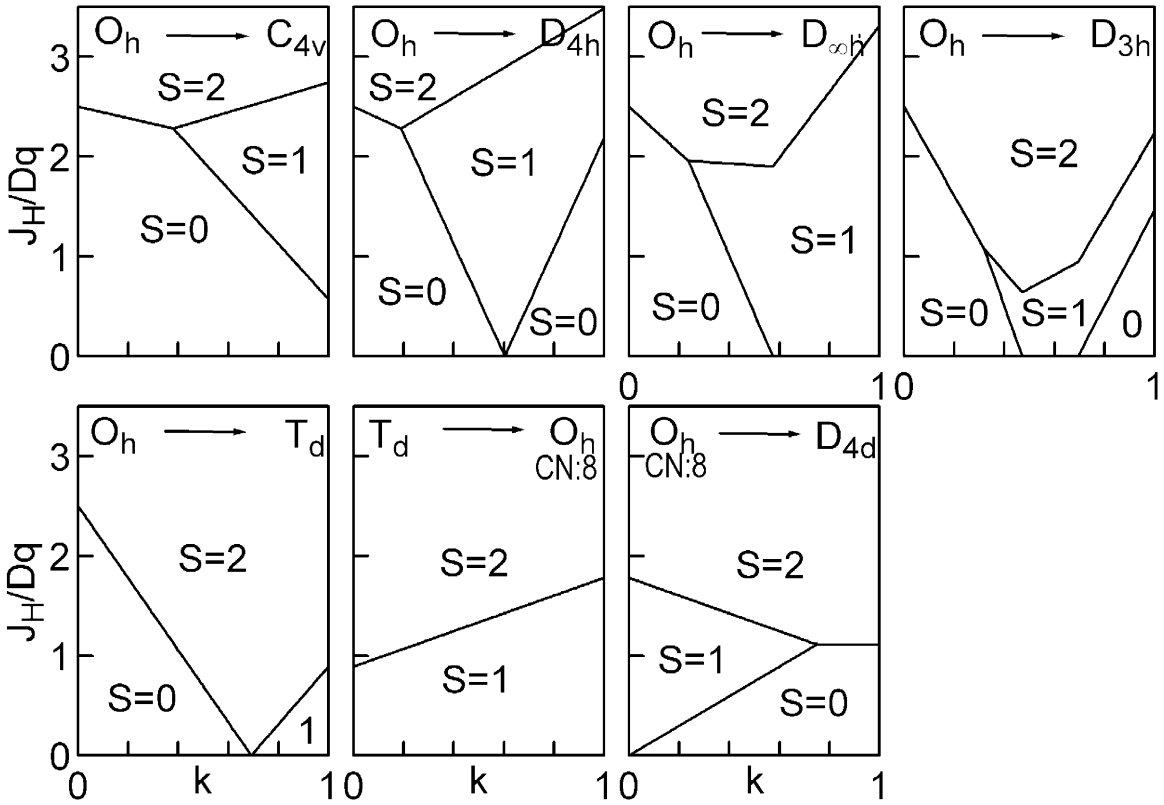

Fig. 6. Spin-state phase diagram for a d^6ion in the various symmetry sites shown in Fig. 2.

depending on the covalence of the bond, J_H values are ranging from 0.6 to 0.9, such spin transitions are expected for *Dq* values ranging from 1.2 to 1.8 eV (i.e. from 2400 to 3600 cm^{-1} ± 25%).

4. Energies of atomic orbitals for d^n (n = 4, 5, 6) ions at the triple point taking into account exchange and correlation

In Fig. 7 we give the orbital splitting for d^n (n = 4, 5, 6) ions at some triple points (t) of the above diagrams (D_{4d}: d^4; C_{4v}: d^5 and d^6) for each of the three spin states.

In each case, we can point out that various orbitals with majority α spin and minority β spin are degenerate. For instance, for a d^6 ion in C_{4v} symmetry, the $d^{\alpha do}_{xy}$ or $d^{\beta do}_{xy}$ orbital from S = 0 is degenerate with $d^{\alpha}_{z^2}$ from S = 1. In the same way, $d^{\beta do}_{xz,yz}$ from S = 1 is degenerate, with $d^{\alpha}_{x^2-y^2}$ from S = 2.

For a band diagram, in the vicinity of the triple point, bands with different symmetry and spin directions will thus overlap.

Hence, starting from S = 1, a spin equilibrium will be described as:

- (*i*) the excitation of an electron from $d^{\beta do}_{xz,yz}$ into (empty) $d^{\alpha}_{x^2-y^2}$ with a spin flip; all the α spin states will be stabilised by $-J_H$ and the energy of the remaining $d^{\beta}_{xz,yz}$ electron will increase by + J_H; in this way we have got the S = 2 (HS) state of Fig. 7;
- (*ii*) the excitation of an electron from $d^{\alpha}_{z^2}$ into $d^{\alpha so}_{xy}$ with a spin flip; it will increase the stability of the β spin states (by $-J_H$); we shall then obtain the S = 0 (LS) state of Fig. 7.

In the case of the d^4 ion, we even observe a degeneracy of the HOMO – including both spin directions –

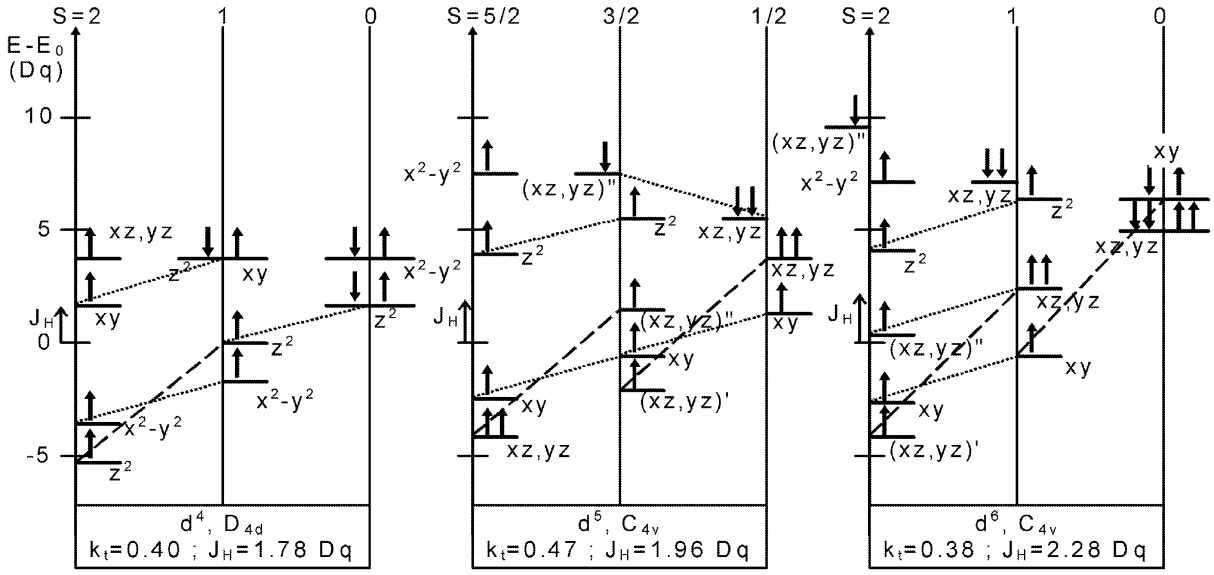

Fig. 7. Atomic orbital energies at the triple point determined in Figs. 4–6 for d^4 in D_{4d}, d^5 and d^6 in C_{4v} symmetry. The origin for the energy scale is $E_0 = 3\,U' - 3\,J_H$, $E_0 = 4\,U' - 4\,J_H$, $E_0 = 5\,U' - 4\,J_H$ for d^4, d^5 and d^6, respectively. Dotted lines and dashed lines indicate J_H and $3\,J_H$ energy differences, respectively. In some cases, ('): singly occupied orbitals, (''): doubly occupied orbitals.

of all the three (S = 0, 1 and 2) spin states simultaneously.

For S = 1, the HOMO itself contain both majority (d^{α}_{xy}) and minority ($d^{\beta}_{z^2}$) spin states.

5. Discussion

5.1. Structural distortions and stabilisation of unusual electronic configurations

5.1.1. d^4 ion

Fig. 4 shows that any distortion of the coordination polyhedron with respect to the O_h (CN = 6) symmetry – with the exception of the prismatic D_{3h} distortion – favours the HS configuration (S = 2). This is the well-known Jahn–Teller effect. On the other hand, a very unusual LS (S = 0) e^4 configuration is favoured in cubic (CN = 8) coordination as well as in triangular prismatic (CN = 6) coordination as a result of the strong stabilisation of the $d_{x^2-y^2}$ and d_{xy} orbitals.

5.1.2. d^5 ion

The usual configurations are HS (S = 5/2) and LS (S = 1/2). An IS (S = 3/2) configuration is possible, especially in C_{4v} and D_{4h} symmetry, and for realistic (close to 2) values of J_H/Dq. This IS configuration could also be associated with a metallic state.

5.1.3. d^6 ion

This is the most favourable number of d electrons for stabilising a LS (S = 0) configuration in an oxygen surrounding as the transition is occurring at J_H/Dq = 2.5, corresponding to the lowest Dq value.

Obviously, the square planar D_{4h} symmetry is the most appropriate for the IS (S = 1) state (see, for instance, [7]) as well as the much more unusual $D_{\infty h}$ (CN = 2) one.

5.2. Exchange, correlation and covalence

U, U' and J_H first are atomic parameters measuring the exchange and correlation effects. As for Racah parameters and particularly B parameter, their values decrease with the hybridisation of metal 3d orbitals with oxygen 2p orbitals, i.e. the covalence of the M–O bond. As we have pointed out earlier [7], the energies of the electrons with majority α spin state are lowered by a value that can reach several times (up to 6 times in some cases) that of J_H, which therefore favours the covalence of the M–O bond, whereas the contribution of electrons with minority β spins is more

Table 2
Exchange and correlation energies for valence electrons of various d^4, d^5 and d^6 configurations.

	HS	IS	LS
d^4	$6\,U' - 6\,J_H - 6\,Dq$	$U + 5\,U' - 3\,J_H - 16\,Dq$	
d^5	$10\,U' - 10\,J_H$	$U + 9\,U' - 6\,J_H - 10\,Dq$	$2\,U + 8\,U' - 4\,J_H - 20\,Dq$
d^6	$U + 14\,U' - 10\,J_H - 4\,Dq$	$2\,U + 13\,U' - 7\,J_H - 14\,Dq$	$3\,U + 12\,U' - 6\,J_H - 24\,Dq$

ionic – the covalent stabilisation is proportional to $\beta^2_{MO}/(H_{ii}(M) - H_{ii}(O))$, where β_{MO} is the resonance integral of the bond and H_{ii} (X) the Coulomb integral of the atom X [8]. This model provides a simple explanation for the high rate of metal-to-ligand hole transfer generally denoted $L(O^-)$ or even $\underline{\underline{L}}(O^0)$ and observed by XAS for ions such as Fe^{4+}, Co^{4+}, Ni^{3+} or Cu^{3+}.

5.3. Exchange, correlation and insulating vs metallic character

The metallic-vs-insulating character of a transition-metal oxide depends on the relative magnitude of the transfer energy β_{MO} or of the bandwidth W and of the so-called Coulomb intra-atomic repulsion $U_{Hubbard}$, corresponding, in an ionic model, to the charge transfer $M^{n+} + M^{n+} \rightarrow M^{(n-1)+} + M^{(n+1)+}$. An upper limit of $U_{Hubbard}$ is then given by the difference between the $(n + 1)$th and nth ionisation energies. Actually $U_{Hubbard}$ and W are not independent and $U_{Hubbard}$ decreases as W increases. The Mott–Hubbard metal–insulator transition is thus governed by the magnitude of the $U_{Hubbard}/W$ ratio.

For a given d^n configuration, it is then important to evaluate the orbital energy of the d^{n+1} configuration for the various possible spin states as a function of U or U', and the type of orbital overlap that controls the value of W and thus the stabilisation due to the transfer. For instance, one sees that for a HS ($S = 5/2$) d^5 ion in C_{4v} symmetry only the HS d^6 configuration involving the π-type $d_{xz,yz}$ orbitals is concerned (Fig. 7), whereas a IS ($S = 3/2$) ion can lead to two possible states $S = 2$ or $S = 1$ of the d^6 configuration. Thus, the insulating-vs-metallic character of a d^n transition metal oxide results from the magnitude of the energy gap separating the d^n from the d^{n+1} configurations.

Confining us to the O_h symmetry and to the above d^5/d^6 case, the following electronic transitions can be considered, in which the type of bonding involved in the charge transfer is given between parentheses:

- (*i*) $d^5_{HS} + d^5_{HS} \rightarrow d^4_{HS} + d^6_{HS}$ (σ, π)
- (*ii*) $d^5_{IS} + d^5_{IS} \rightarrow d^4_{IS} + d^6_{HS}$ (σ)
- (*iii*) $d^5_{IS} + d^5_{IS} \rightarrow d^4_{HS} + d^6_{IS}$ (π)
- (*iv*) $d^5_{LS} + d^5_{LS} \rightarrow d^4_{IS} + d^6_{LS}$ (π)

and for each of them we can calculate the energy gaps using the total energies including exchange, correlation and crystal field contributions for all the valence electrons (Table 2).

With the exception of (*i*), all the transfers correspond to a minimal energy of $U' - J_H$. For the first case, the gap ($U' + J_H$, assuming $J_H/Dq = 2$) is less favourable to such a transfer.

However, only (*ii*) involves σ-type bands that are broader than π-type ones. The ratio $(U' - J_H)/W_\sigma$ is then the most favourable for the formation of a metallic state from an IS state.

In the case of a lower symmetry favouring the HS↔IS spin equilibrium (Fig. 5), it should be noticed that case (*i*) can be split into two steps:

- (*i'*) $d^5_{HS} + d^5_{HS} \rightarrow d^5_{IS} + d^5_{HS}$
- (*i''*) $d^5_{IS} + d^5_{HS} \rightarrow d^4_{HS} + d^6_{HS}$ (σ)

and the gap corresponding to (*i''*) is equal to U'.

This HS/IS configuration mixing could also lead to a metallic state, as it implies a σ-type transfer.

This simple ionic-type approach of exchange and correlation explains the insulating behaviour of $LaFeO_3$and of $LaCoO_3$ at low temperature as well as the transition to a metallic behaviour at high temperature for the latter.

Indeed, for Fe^{3+} in $LaFeO_3$, the J_H/Dq ratio, much larger than 2.5, favours the exchange energy gain with respect to the crystal field and leads to a HS ($t_{2g}^{\alpha 3}\, e_g^{\alpha 2}$) state. The upper Hubbard band corresponding to the HS ($t_{2g}^{\alpha 3}\, e_g^{\alpha 2}\, t_{2g}^{\beta 1}$) d^6 configuration lies at a much higher energy than the lower Hubbard band and is well separated from it, which accounts for the insulating character.

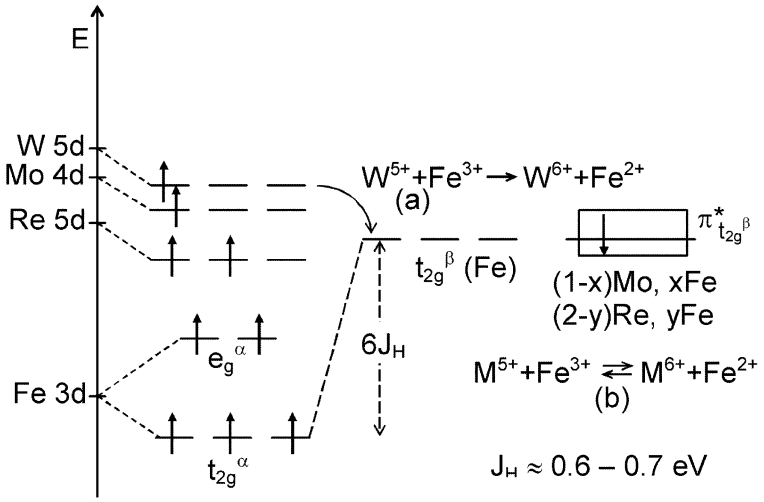

Fig. 8. M^{5+}/Fe^{3+}charge transfer in Sr_2FeMO_6 (M = Mo, W, Re) perovskites.

On the other hand, in $LaCoO_3$, Co^{3+} is in a LS ($t_{2g}^6\ e_g^0$) state at low temperature and thus insulating, because the crystal field energy overcomes the exchange contribution. As the temperature increases, the Co–O distances become longer, leading to a decrease of the covalence and of *Dq*, and the exchange and correlation parameters slightly increase, which leads to a change in the electronic configuration. $LaCoO_3$ was first described as undergoing a LS($S = 0$)↔HS($S = 2$) transition [9]. Recent works now describe the transition as LS($S = 0$)↔IS($S = 1$), which better agrees with our description of the insulator to metal transition given above [10, 11]. Double perovskites synthesised several decades ago such as Sr_2FeMoO_6 (M = Mo, W, Re...) and characterised by very different physical properties (either ferromagnetic metal or antiferromagnetic insulator) depending on the nature of M, are now revisited, since giant magnetoresistance has been observed for these materials [12]. If we consider the possibility of a charge transfer between M^{5+} and Fe^{3+} ions such as:

$$M^{5+} + Fe^{3+} \rightarrow M^{6+} + Fe^{2+}$$

we have to compare the energy of iron d orbitals ($E_{Fe:3d} = -16.5$ eV) modified by crystal field, exchange and correlation effects ($t_{2g}^{\beta do}$ of Fe^{2+} is shifted by 6 J_H above $t_{2g}^{\alpha so}$) with that of M^{5+} ions orbitals (Mo^{5+}: $4d^1$, W^{5+}: $5d^1$, Re^{5+}: $5d^2$), the energies of which depend on the main quantum number *n* and atomic number *Z* ($E_{Mo:4d} = -11.5$ eV, $E_{W:5d} = -11.0$ eV, $E_{Re:5d} = -12.3$ eV) (Fig. 8).

We now understand why a partial transfer is possible in the molybdenum and rhenium cases: a $\pi^*(t_{2g}^{\beta})$ band of the Fe–Mo(Re)–O type involving mixed valences Fe^{III}/Fe^{II} and Mo^{V}/Mo^{VI} gives rise to a metallic character and strong ferromagnetic interactions between localised iron moments via the itinerant $\pi^{*\beta}$ electrons accounting for a high T_c value.

The highest energy of tungsten 5d orbitals leads to a complete charge transfer, giving single valence $Fe^{2+}(3d^6)$ and W^{6+} ($5d^0$) ions, resulting in an insulating character and weak antiferromagnetic interactions ($T_N \approx 20$ K) between Fe^{2+} ions.

6. Conclusions

In order to clarify the competition of exchange and correlation energies vs crystal field stabilisation energy, a simple approach is proposed. The exchange and correlation contributions have been described on the base of Brandow and Kanamori's *U*, *U'* and J_H parameters. The dependence of the crystal field on site distortion has simply been modelled using a linear interpolation between undistorted and fully distorted site. This approach led to establish phase diagrams for d^4, d^5 and d^6 cations, allowing us to predict the spin-state stability range depending on exchange (J_H), crystal field (*Dq*)

and distortion (k) parameters. It can be used to complement the Extended Hückel Tight Binding calculations of the electronic structure of materials with a noticeable ionic character such as 3d transition-metal oxides, in order to interpret their electronic behaviour and, particularly, discuss their insulating-vs-metallic character, as we recently did [13].

References

[1] C. Cohen-Tannoudji, B. Diu, F. Laloë, Mécanique quantique, tome II, Hermann, Paris, 1998, p. 1410; J.D. Morgan III, W. Kutzelnigg, J. Phys. Chem. 97 (1993) 2425.
[2] V.I. Anisimov, J. Zaanen, O.K. Andersen, Phys. Rev. B 44 (1991) 943.
[3] E. Clementi, D.L. Raimondi, J. Chem. Phys. 38 (1963) 2686.
[4] J. Kanamori, J. Phys. Chem. Solids 10 (87) (1963).
[5] J. Brandow, Adv. Phys. 26 (1977) 651.
[6] R. Krishnamurthy, W.B. Shaap, J. Chem. Educ. 46 (1969) 799.
[7] M. Pouchard, A. Villesuzanne, J.P. Doumerc, J. Solid State Chem. 162 (2001) 282.
[8] W.E. Pickett, D.J. Singh, Phys. Rev. B 53 (1996) 1146.
[9] J.B. Goodenough, Progr. Solid State Chem. 5 (1971) 145.
[10] M.A. Señaris-Rodriguez, J.B. Goodenough, J. Solid State Chem. 116 (1995) 224.
[11] M.A. Korotin, S.Y. Ezhov, I.V. Solovyev, V.I. Anisimov, D.I. Khomskii, G.A. Sawatzky, Phys. Rev. B 54 (1996) 5309.
[12] S. Ray, A. Kumar, S. Majumdar, E.V. Sampathkumaran, D.D. Sarma, J. Phys.: Condens. Mat. 13 (2001) 607.
[13] M.H. Whangbo, H.J. Koo, A. Villesuzanne, M. Pouchard, Inorg. Chem. 41 (2002) 1920.